Asian Journal of Chemistry; Vol. 25, No. 17 (2013), 9601-9604

ASIAN JOURNAL OF CHEMISTRY

http://dx.doi.org/10.14233/ajchem.2013.15093

# Optical Properties of Indium-Doped ZnO Nano-Films Prepared by Spray Pyrolysis and Hydrothermal Synthesis

RUXI LIU, ZHONG ZHANG*, JINZHAO HUANG and HONGLIN LI

School of Physics Science, University of Jinan, Jinan 250022, Shandong Province, P.R. China

*Corresponding author: Tel: +86 15168808080; E-mail: ss_zhangz@ujn.edu.cn

(*Received*: 4 January 2013; *Accepted*: 7 October 2013) AJC-14236

Zinc oxide and indium-doped ZnO nano-films are prepared by two-step method on the quartz glass substrate. The growth orientation along c-axis of ZnO nano rods is changed by indium doping and with the increase of indium proportion, the orientation along (101) plane increase. The structure changes from prism-like nano rods to nanofilms due to the different indium proportion. New energy levels are introduce into ZnO causing a blue shift in the green emission region and more oxygen vacancies that results a better blue emission at 404 nm.

**Key Words: Zinc oxide, Spray pyrolysis Method, Hydrothermal synthesis method, Indium doping, Nano structure.**

## INTRODUCTION

Zinc oxide is a research hotspot of the 3rd generation semicondutor with a wide bandgap energy (3.37 eV) and a large excitation binding energy (60 meV) at room temperature. Nanoscale ZnO structures are different from bulk materials due to quantum scale effect as the result of that their increased surface area and they show their favourable structural, optical and catalytic properties. Zinc oxide nano structures are often used as light-emission diode[1], gas sensors[2], antireflective coating[3], photocatalyst[4] and in solar cells[5].

The synthesis of ZnO nano structure have been carried out using chemical methods such as sol-gel method[6], metal-organic chemical vapor deposition (MOCVD)[7], thermal evaporation deposition[8], electrochemical deposition[9], hydrothermal method[10], magnetron sputtering method[11] and anodic alumina templates *etc*.[12] and physical methods as pulsed laser deposition (PLD)[13] and molecular beam epitaxy (MBE), *etc*.[14].

The undoped ZnO films are not very stable especially at high temperatures, but the doped ZnO films can reduce the disadvantage and increase the conductivity. Though doping can improve the quality of ZnO films, the efficiency of the dopant element depends on its electronegativity and difference between its ionic radius and the ionic radius of zinc[15]. Most indium doped ZnO films are prepared by spray pyrolysis[2,15]. In this paper, the ZnO and indium-doped ZnO nano-films are prepared by two-step method using different indium concentrations at [In]/[Zn] = 3, 5, 8, 10 at %. The ZnO seeds layer is prepared on the substrates by spray pyrolysis firstly and then the indium-doped ZnO nano-films are prepared by hydrothermal synthesis.

## EXPERIMENTAL

Materials used in the experiment were quartz glass, zinc acetate, ammonia, indium chloride, zinc nitrate hexahydrate and hexamethlylenetetramine. The methods employed for indium doped ZnO nano films were spray pyrolysis and hydrothermal synthesis.

**General procedure:** The seeds layer is prepared by spray pyrolysis on the quartz glass at 300 ºC with 0.5 M zinc acetate. The ZnO growth solution is prepared by dropping ammonia to the solution of zinc nitrate hexahydrate and hexamethlylenetetramine till it turns to transparent. Then the substrate is put into the solution vertically in the autoclave. The final growth is carried out at 100 ºC and the time of 2 h. By dissolving different weight indium chloride also to the solution of zinc nitrate hexahydrate and hexamethlylenetetramine and repeating final growth process as ZnO nano-films, the indium-doped ZnO nano-films are prepared. All the samples prepared are annealed at 300 ºC to 0.5 h, then quenched to the room temperature and finally cleaned by ethanol and deionized water before tested.

**Detection method:** The as-grown films are tested by the X-ray diffraction (XRD), the scanning electron microscopy (SEM), the photoluminescence (PL) and current-voltage characteristics curves (I-V) to indicate the influence of indium-doping to ZnO nano-films.

## RESULTS AND DISCUSSION

Fig. 1 shows the XRD patterns of ZnO and indium-doped ZnO nano-films. All the diffraction peaks in each patterns consistent with the standard card (JCPDS card 36-1451), which

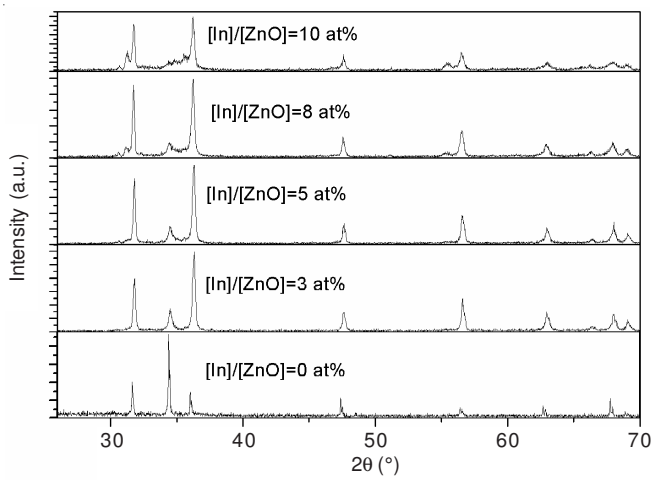


Fig. 1. XRD patterns of ZnO and indium-doped ZnO nano-films

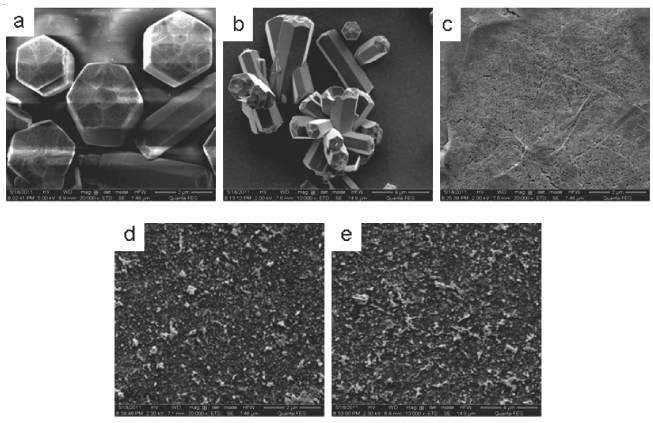


Fig. 2. SEM images of ZnO and indium-doped ZnO nano-films. (a) prism-like nano rod structure of ZnO, (b) flower-like stucture of ZnO at 3 % of indium proportion, (c) nano-films of ZnO at 5 % of indium proportion, (d) nano-films of ZnO at 8 % of indium proportion and (e) nano-films of ZnO at 10 % of indium proportion

represents the wurtzite structure of ZnO. Compared to none indium-doped ZnO nano-films, the c-axis orientation along the (002) plane decrease with the increase of indium proportion and the peak of orientation along (101) plane increase, when the indium proportion up to 10 %, the diffraction peak of (002) plane almost disappears, all above indicate that the growth orientation of the ZnO crystal is obviously influenced by the incorporation of indium. The ionic radius of indium is more than the zinc ionic radius, so that the lattice expands and the lattice parameters increase when indium ionic replaces Zn ionic in the ZnO lattice, resulting a shift to the small angle direction of the diffraction peaks of (100), (002) and (101) plane of indium-doped ZnO nano-films compared to the standard card and the change of the distance of the two crystal plane is $3.5 \times 10^{-3}$ nm. Diffraction peaks of the patterns from ZnO to indium-doped ZnO at 10 % nano-films become wider, indicating a lower crystallinity and smaller average grain size which can be corroborated by Scherer Formula (the calculated average grain sizes are 2.144976, 1.244333, 1.190992, 1.052201 and 1.211128 nm, respectively). The pattern of 8 % indium proportion shows a new peak on the left of the (100) plane peak indicating the diffraction peak of $In_2O_3$ and it is stronger in the pattern of the 10 % indium proportion. The peak of $In_2O_3$ indicates that not all Zn ionics are replaced by indium ionics, but some indium ionics form $In_2O_3$ in the wurtzite structure of ZnO.

Fig. 2 are the SEM images showing the morphology of indium-doped ZnO nano-films. Fig. 2(a) shows the wurtzite structure of ZnO nanorods that is prism-like. Most nanorods grow vertically from the substrate mostly and few grow along the horizontal direction. The bottom of the rods is thinner than the upper indicating that the rod structure is grown from the seed layers and the preferential growth direction of the seed layers decides the growth direction of the rods, so that the nanorods grow along different direction. Fig. 2(b) is the flower-like nano structure image of indium proportion at 3 %. The flower-like structure is the result of the distorted rod-like structure and there are fluffs formed on the surface of the rods and the rod structure becomes being deform caused by the indium doping, the complete rod structure in the upper left corner indicates that small amount indium ionic are doped into the ZnO structure. Fig. 2(c-e) are the images of different indium doping proportion ZnO nano-films at 5, 8 and 10 %, respectively. The surface of the nano-films becomes irregular with the increase of indium proportion and the growth direction changes instead of along the c-axis mainly indicating that the wurtzite structure of ZnO deforms due to the doping of indium in the growth progress. The SEM images consistent to the XRD patterns that the growth orientation changes remarkably.

Fig. 3 shows the photoluminescence emission spectra of the samples. The photoluminescence peaks are attributed by a 325 nm excitation from LS55 fluorescence spectrophotometer of Perkin Elmer company. After indium doping, the visible luminescence intensity of nano-films became higher and entirely intensity became lower than ZnO nano-structure, this depends on sample type and excitation intensity[16].

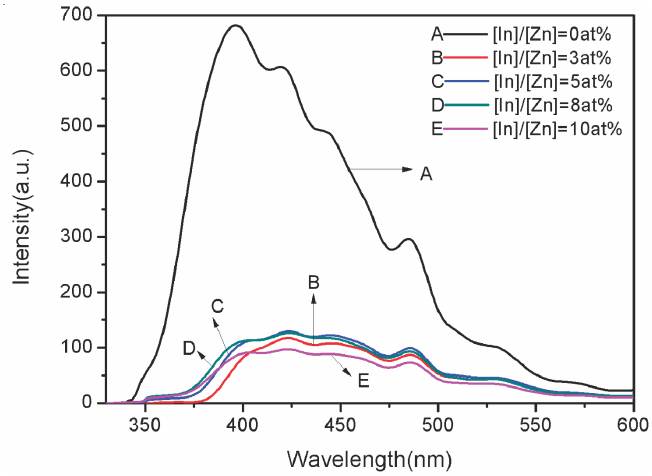


Fig. 3. Photoluminescence sectra of ZnO and indium-doped ZnO nano-films

The photoluminescence spectra are Gaussian deconvoluted to the sub peaks according to their origination to investigate deep of the photoluminescence spectra, showed as Fig. 4.

The UV emission at 388 nm is assigned to a shallow donor of the complex defect of $Zn_i$[17] and also the peak at 421 nm[18]. The peaks at 489 and 520 nm are mostly attriburted to $V_O$[19] and $O_{Zn}$[20], respectively. The peaks that are bigger than 540 nm are ascribed to $O_i$[21].

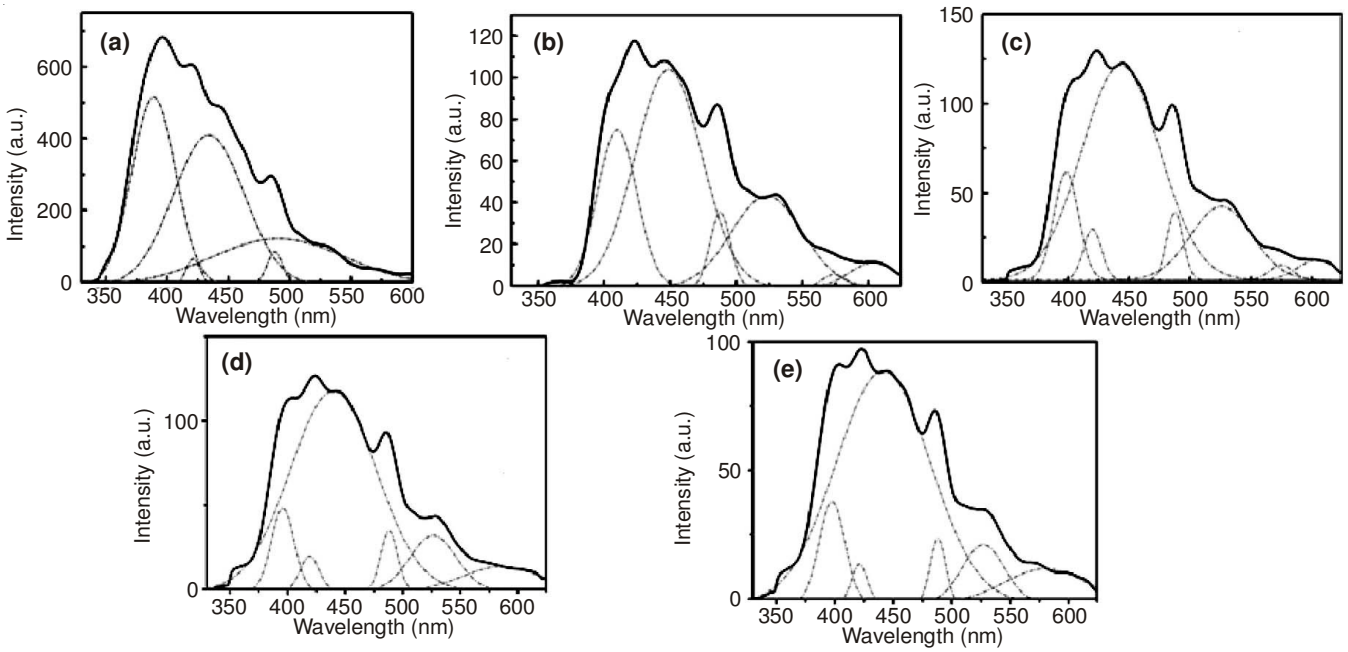


Fig. 4. Gaussian deconvolution of photoluminescence spectra of: (a) nano structure ZnO, (b) nano structure of ZnO at 3 % of indium proportion, (c) nano-films of ZnO at 5 % of indium proportion, (d) nano-films of ZnO at 8 % of indium proportion and (e) nano-films of ZnO at 10 % of indium proportion. The main considerations in Gaussian deconvolution are: the peaks are relatively fixed; all peaks are considered; relatively high correlation coefficient ($r^2 > 0.99$)

According to reference[22] and by the equation:

$$E = h \times \nu = h \times \frac{c}{\lambda}$$

we calculated and drew the band-gap energy of ZnO nano-films and defects such as oxygen vacancy ($V_O$), zinc vacancy ($V_{Zn}$), interstitial zinc and interstitial oxygen and new energy levels(NV) introduced by indium doping showed as Fig. 5.

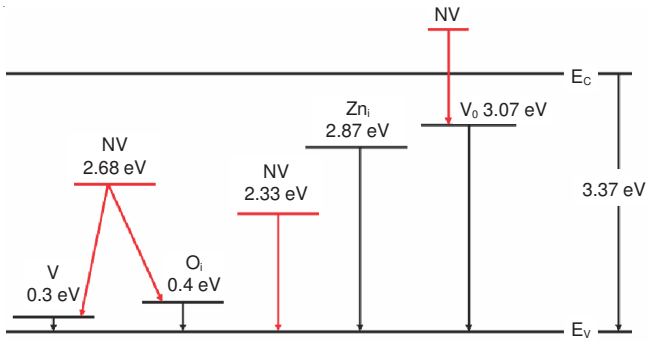


Fig. 5. Energy levels of indium-doped ZnO nano-films

From calculation, the nano-films band gap energy is 3.14 eV, less than the general one of 3.37 eV, caused by poor crystalline quality. The ultraviolet emission peak of ZnO and indium-doped ZnO nano-films at 396 and 404 nm are caused by the transition of electrons from conduction band to valence band and transition to $V_O$ level respectively. The red shift of the UV-emission peak from ZnO and indium-doped ZnO nano-films is the result of the increase of $V_O$ level that covers up the character emission peak of ZnO and the indium doping made lattice constant bigger than nano ZnO resulting a less band gap energy. There are three emission peaks of 423, 445 and 486 nm in the blue region of all the spectra are the results of transition from conduction band to $V_{Zn}$, from $V_O$ to $V_{Zn}$ and from $Zn_i$ to $V_{Zn}$ respectively according to the calculation. There is a blue shift of the green region (changing from 535-534, 532, 531 and 529 nm that from ZnO to indium-doped ZnO of the indium proportion 3, 5, 8 and 10 %, respectively) and increased intensity showed in Fig. 4 and the green emission is ascribed to the transitions from deep level to the $V_O$ level, so by calculation the blue shift can be explained that the increase and the different surrounding of the oxygen vacancies and the transitions of the three possible new energy levels caused by incorporation of indium ionics into the wurtzite structure of ZnO and the new energy levels moves to higher energy level with the increase of indium doping.

So that the result of indium-doped ZnO nano-films is that the emission peaks shift to the middle wavelength from UV and green region.

## Conclusion

ZnO and indium-doped ZnO nano-films are prepared by a new two-step method on the quartz glass substrates. The zinc acetate solution is ultrasonic sprayed on the substrates at 300 °C to prepared ZnO seed layers. The growth orientation of ZnO nano films chenges from along c-axis to (101) plane with the increase of indium proportion. ZnO nano rods films are prepared by the method. The structure changes from prism-like nano rods to nanofilms due to the different indium proportion indicating that the dopant distorts the wurtzite structure of ZnO because of the different ionic radius. New energy levels are introduce into ZnO. The increase of indium doping causes a blue shift in the green emission region and the increase and change of chemical surroundings around oxygen vacancies result a better blue emission at 404 nm.

## ACKNOWLEDGEMENTS

The authors thank for the support of the National Natural Science Foundation of China (Grant No. 61106059, 61172028), the Encouragement Foundation for Excellent Middle-aged and Young Scientist of Shandong Province (Grant No. BS2011NJ003), the Science-Technology Program of Higher Education Institutions of Shandong Province (Grant No. J11LA10), the Doctoral Foundation of University of Jinan (Grant No. XBS0845), Shandong Foundation for Development of Science and Technology (Grant No. 2009GG20003028, 2010GG0020423).

## REFERENCES

1. J. Sun, Q. Feng, J. Bian, D. Yu, M. Li, C. Li, H. Liang, J. Zhao, H. Qiu and G. Du, *J. Lumin*., **131**, 825 (2011).
2. R. Ferro, J.A. Rodríguez and P. Bertrand, *Thin Solid Films*, **516**, 2225 (2008).
3. Y.J. Lee, D.S. Ruby, D.W. Peters, B.B. Mckenzie and J.W.P. Hsu, *Nano Lett.*, **8**, 1501 (2008).
4. T. Szabo, J. Nemeth and I. Dekany, *Colloids Surf. A*, **230**, 23 (2003).
5. M. Krunks, A. Katerski, T. Dedova, I. Oja Acik and A. Mere, *Sol. Energy Mater. Sol. Cells*, **92**, 1016 (2008).
6. D.T. Phan and G.S. Chung, *Appl. Surf. Sci*., **257**, 3285 (2011).
7. A. Marzouki, A. Lusson, F. Jomard, A. Sayari, P. Galtier, M. Oueslati and V. Sallet, *J. Cryst. Growth*, **312**, 3063 (2010).
8. J.H. Zheng, Q. Jiang and J.S. Lian, *Appl. Surf. Sci*., **257**, 5083 (2011).
9. G. He and K. Wang, *Appl. Surf. Sci*., **257**, 6590 (2011).
10. S. Kerli, U. Alver, H. Yaykasli, B. Avar, A. Tanriverdi and C. Kursun, *Asian J. Chem.*, **25**, 7539 (2013).
11. X. Bie, J. Lu, Y. Wang, L. Gong, Q. Ma and Z. Ye, *Appl. Surf. Sci*., **257**, 6125 (2011).
12. Q. Wang, G. Wang, B. Xu, J. Jie, X. Han, G. Li, Q. Li and J.G. Hou, *Mater. Lett*., **59**, 1378 (2005).
13. W. Zhaoyang, S. Liyuan and H. Lizhong, Vacuum, 85, 397 (2010).
14. S.C. Su, Y.M. Lu, Z.Z. Zhang, C.X. Shan, B. Yao, B.H. Li, D.Z. Shen, J.Y. Zhang, D.X. Zhao and X.W. Fan, *Appl. Surf. Sci*., **254**, 7303 (2008).
15. P. Nunes, E. Fortunato, P. Tonello, F. Braz Fernandes, P. Vilarinho and R. Martins, *Vacuum*, **64**, 281 (2002).
16. W.S. Shi, B. Cheng, L. Zhang and E.T. Samulski, *J. Appl. Phys*., **98**, 083502 (2005).
17. D.C. Look, J.W. Hemsky and J. Sizelove, *Phys. Rev. Lett*., **82**, 2552 (1999).
18. M.K. Lee and H.F. Tu, *J. Appl. Phys*., **101**, 12603 (2007).
19. W. Cheng, P. Wu, X. Zou and T. Xiao, *J. Appl. Phys*., **100**, 054311 (2006).
20. C.-H. Tsai, W.-C. Wang, F.-L. Jenq, C.-C. Liu, C.-I. Hung and M.-P. Houng, *J. Appl. Phys*., **104**, 053521 (2008).
21. S.A. Studenikin, N. Golego and M. Cocivera, *J. Appl. Phys*., **84**, 2287 (1998).
22. P.S. Xu, Y. Sun, C. Sun and F.Q. Xu, *Sci. China (Series A)*, **31**, 358 (2001).